Natural Resources for Human Health
eISSN: 2583-1194

Original Research

Received 18 May 2026
Revised 22 June 2026
Accepted 10 July 2026

Natural Resources for Human Health 2026, Vol. 6 (6s): 1093–1112

KEYWORDS:
Shatt Al-Arab River, Water Quality, Geographic Information Systems (GIS), Remote Sensing, Electrical Conductivity, Total Dissolved Solids, Turbidity, pH, Landsat 8.

Spatial and Seasonal Distribution of Shatt Al-Arab Water Quality Using Geographic Information Systems: Variations in Salinity, Turbidity, and pH

Sadiq Jaafar Talib AL-Mousawi, Najla Jabr Mohammed AL-Amiri, Mohammed Ahmed Kadhim AL-Hayali

Department of Soil Sciences and Water Resources, College of Agriculture, University of Basrah, Basrah, Iraq

ABSTRACT: The current research attempted to assess the spatial and seasonal variations in some water quality parameters in Shatt Al-Arab River by applying Geographic Information System (GIS) techniques in conjunction with remote sensing technology. Landsat 8 satellite images acquired from the United States Geological Survey (USGS) database were applied to evaluate the spatial distribution of the parameters including pH, electrical conductivity (EC), total dissolved solids (TDS), and turbidity.

Twenty-nine sampling stations were set up in the River stretching from the northern station at Al-Sharash to the southern station at Al-Wasiliyah Port. The water sampling and analysis processes took place during one year from November 2024 to October 2025.

According to the results, it was found out that the pH values ranged between 7.0 and 8.6, while the monthly average varied from 7.7 to 7.9, indicating a lack of spatial variation among the stations. On the other hand, EC and TDS revealed a clear longitudinal trend. The quality of the river waters changed from slightly saline water in the northern part of the River to highly saline in the southern part, and exceeded seawater salinity in some stations of the southern part during summer and autumn seasons. Moreover, the TDS values experienced marked seasonal changes and increased gradually towards the middle and southern parts of the River.

In addition, the turbidity experienced significant spatial and seasonal variations. The minimum turbidity values were measured in autumn, whereas the maximum turbidity values were observed in summer. Using GIS for the spatial analysis made it possible to detect water quality deterioration areas. Moreover, it was shown that there is a significant deterioration of water quality in the estuarine zone in terms of salinity and turbidity.

Thus, the present research proves the applicability of GIS and remote sensing techniques in assessing the spatial and temporal variations of river water quality.

1. INTRODUCTION:

The Shatt Al-Arab River plays an important role as the major surface river in Iraq and it is the main source of surface water for the Basrah Governorate. It is highly essential for domestic, agricultural, industrial, economic, environmental and recreational uses (Moyel, 2014). However, there have been some significant changes in its hydrological characteristics and water quality in recent decades resulting from low freshwater inflows, climatic change, water management activities upstream and increasing anthropogenic impacts.

There have been several studies on the degradation of the water quality of the Shatt Al-Arab, especially in terms of salinity, electrical conductivity (EC) and chloride content, making it unsuitable for agricultural and domestic applications (Al-Essa, 2004). One of the key water quality parameters is pH, indicating the acid-base status of the aquatic environment, which is impacted by the presence of industrial effluents, agricultural drainage, domestic sewage, atmospheric deposition and biological processes. Natural waters usually have pH levels between 6.5 and 8.5 (Al-Aboodi et al., 2018).

Natural Resources for
Human Health
eISSN: 2583-1194

Several earlier studies showed that the waters of the Shatt Al-Arab River have slightly alkaline pH levels. According to Al-Asadi et al. (2020), pH levels vary between 7.86 at Al-Qurnah and 8.07 at Al-Faw. The same results have been obtained by Al-Amiri and Disher (2021), Al-Bazouni (2023), Al-Zubaidi (2023), Mehasin et al. (2025) and Hamzah (2025), who observed alkaline pH conditions in the river.

The EC and TDS levels are commonly used as the indicators of the salinity and mineralization of the waters. According to Adlan (2022), there have been significant spatial and temporal differences in EC levels in the Shatt Al-Arab River, varying between 1.62 dS m^{-1} at Al-Qurnah and 10.15 dS m^{-1} at Ras Al-Bisha. The same increase in EC levels was detected by Jassim and Al-Amiri (2023) from north to south stations up to 28.8 dS m^{-1} in the estuarine area. There have also been considerable spatial differences in TDS levels in the Shatt Al-Arab River. Al-Ghalibi and Al-Saadi (2019) reported that the mean TDS levels varied between 1.48 g L^{-1} at Al-Qurnah and 23.416 g L^{-1} at Al-Faw. The same tendency was found by Al-Noor (2021) and Al-Bazouni (2023) with increasing salinity in the south part of the river due to seawater intrusion and low freshwater discharge.

Turbidity is also one of the key water quality parameters indicating the amount of suspended and colloidal matter in the water. High turbidity makes the water less transparent, impacting aquatic ecosystems and reducing the suitability of water for domestic and industrial use (WHO, 2018; Qzar et al., 2021; Mohammed et al., 2022). Several previous studies have found a significant increase in turbidity in the southern part of the river, especially near Al-Naqaa and Ras Al-Bisha stations (Adlan, 2022; Al-Zubaidi, 2023).

Geographic Information Systems (GIS) can be considered as one of the most effective tools for water resources assessment and environmental monitoring. The GIS allows storing, analyzing, visualizing and updating spatial data, helping to support decision-making processes in water resources management (Jabber, 2012). Several studies have demonstrated the effectiveness of GIS in the evaluation of the spatial and temporal distribution of the water quality parameters and pollution hotspots identification (Mohamed et al., 2016; Al-Hashmi et al., 2023).

Hence, the current research aims at the assessment of the spatial and seasonal distribution of selected water quality parameters along the Shatt Al-Arab River using GIS and remote sensing methods.

2. STUDY AREA

The study area is represented by the Shatt Al-Arab River that starts from Al-Qurnah District located in the northern part and ends at Al-Faw District in the southern part of south Iraq. In total, twenty-nine sampling locations were chosen on the river, starting from Al-Sharash (Shallahat Al-Hassan region) and ending at Al-Wasiliyah Port. Consequently, the distance between these two points is equal to 121.723 km. The geographical location of the study area ranges from longitudes 47°28'21"E and 48°16'50"E to latitudes 30°19'29"N and 30°57'24"N. Figure 5 presents the geographical location of the study area and the distribution of sampling stations

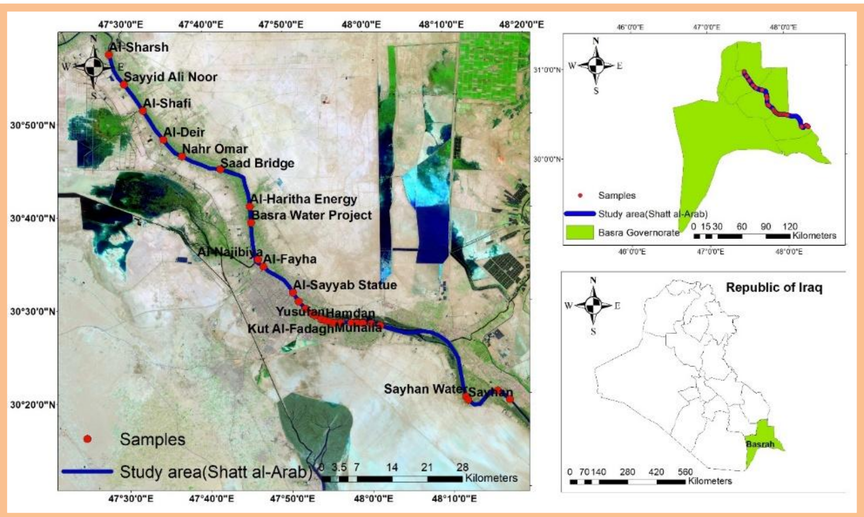

Figure 1. Location of the Study Area

MATERIALS AND METHODS

Field Survey and Sampling Stations

Different field reconnaissance and survey missions were carried out on the Shatt Al-Arab River to determine appropriate sampling points. The geographic coordinates of the sampling stations were established through GPS, as indicated in Table 1, and later projected on maps based on the Universal Transverse Mercator (UTM) coordinate system.

Various factors were taken into consideration when selecting the sampling sites, such as geographical location along the river, accessibility, proximity to human and agricultural settlements, as well as water desalination plants, in order to ensure that all environmental conditions of the Shatt Al-Arab River were represented in the research.

Water samples were taken depending on the date of acquisition of the Landsat 8 satellite images. One-year-long sampling took place between October 30, 2024 and October 17, 2025. The collected samples were then preserved in clean one-liter polyethylene bottles and stored in cooled boxes up to the time of laboratory analysis.

Remote Sensing Data Processing

Remote sensing data used in this study were obtained from the website of the United States Geological Survey (USGS). The first Landsat 8 image of the study area was acquired on October 30, 2024, followed by other images during the study period with the last one acquired on October 2, 2025. The compressed data set of each Landsat 8 image had eleven spectral bands. Spatial resolution was 30 m × 30 m for Bands 1 – 7 and 9, 100 m × 100 m for Thermal Bands 10 and 11, while that of Panchromatic Band 8 was 15 m × 15 m.

Image processing included the use of radiometric and geometric corrections before carrying out any further analysis. The spectral bands related to the Operational Land Imager (OLI) sensor were processed and compiled in ArcMap 10.4.1 software. These comprised Band 2 (Blue), Band 4 (Red), and Band 7 (Shortwave Infrared-2) in order to create an image that was ready for digital image processing and classification.

Geographic Information System (GIS) Analysis

GIS analysis involved georeferencing, digitizing, building the database, and thematic mapping of water quality parameters and sampling points. This was done using the software ArcGIS 10.4.1. GIS system allowed data to be entered, stored, retrieved, analyzed and used in combination of spatial and attribute databases. Moreover, GIS was used for making maps, charts, and tables for interpreting the results.

Water Quality Analysis

The chemical characteristics of water samples were determined according to the standard methods described in APHA (2017).

pH The pH of water samples was measured using a JENWAY 3505 pH meter.

Electrical Conductivity (EC) Electrical conductivity was determined using a JENWAY 4510 conductivity meter, and results were expressed as dS m^{-1}.

Total Dissolved Solids (TDS) Total dissolved solids were measured directly using a JENWAY 4510 conductivity meter and expressed as mg L^{-1}.

Turbidity Turbidity was measured using a Lovibond Turbidity Meter, and the results were expressed in Nephelometric Turbidity Units (NTU).

Table 1. Geographic Coordinates and Locations of Water Sampling Stations along the Shatt Al-Arab River

Station number	Station name	Geographic coordinates(UTM)	
		Longitude	Latitude
S1	Al-Sharsh	736156.614	3427494.352
S2	Sayyid Ali Noor	739253.784	3421511.238

S3	Al-Shafi	742741.377	3416230.709
S4	Al-Deir	747012.936	3410594.887
S5	Nahr Omar	750757.16	3407218.06
S6	Saad Bridge	758465.469	3404716.441
S7	Al-Haritha Energy	764116.621	3397296.782
S8	Basra Water Project	764443.914	3394106.992
S9	Al-Najibiya	765244.345	3386447.145
S10	Al-Fayha	766995	3385602.544
S11	Al-Sayyab Statue	772687	3380045.756
S12	Al-Ta'leemi Hospital	773866.457	3378415.193
S13	Awaisiyan	775237.042	3376944.287
S14	Fajjat Al-Arab	776607.216	3375917.894
S15	Mahjaran	777078.648	3375594.373
S16	Yusufan	778349.174	3374921.609
S17	Hamdan	779322.835	3374540.005
S18	Kut Al-Fadagh	780089	3374311.346
S19	Muhaila	781126.733	3374163.16
S20	Al-Sankar	782383.477	3374120.083
S21	Abu Mughira	784412.02	3374075.832
S22	Nahr Khuz	785449.774	3374048.935
S23	Al-Labani	786692.511	3374042.547
S24	Al-Sahel	212283.717	3373823.469
S25	Abu Flous Port	214004.767	3373424
S26	Sayhan Water	230127.399	3358542.453
S27	Sayhan	230508.443	3357831.47
S28	Al-Siba	236610.792	3359302.866
S29	Al-Wasiliya	238828.425	3357499.221

RESULTS AND DISCUSSION

1. Potential of Hydrogen (pH)

As seen from the data in Table 2, the pH value in the water samples of Shatt Al-Arab was mostly in the range of 7.0-8.6, with mean pH values ranging between 7.7 and 7.9 per month. This pH falls under the normal range of fresh to moderately saline water according to WHO and FAO.

In general, most of the sampling sites showed some slight alkalinity characteristic of surface water that contains calcium and magnesium bicarbonates (Al-Taher, 2019). This led to little variation in the pH levels of the different stations sampled. The results were consistent with those reported by Al-Asadi et al. (2020) and Hamzah (2025).

2. Spatial Distribution of pH Values During the Seasons

Figure 2 shows the influence of seasonality on the pH values in Shatt Al-Arab River. According to the results obtained, the system was characterized by a relatively stable, slightly alkaline state with minor spatial and temporal variations due to high buffering capacity of the river water.

The higher pH values were found in the summertime and autumn with pH varying from 7.66 to 8.23 and 7.37 to 8.23, respectively. The reasons for the increase in pH levels may include higher temperatures and increased evaporation in the summer and autumn seasons. Also, these seasons are characterized by reduced discharge of freshwater into the Shatt Al-Arab River leading to lower flow and longer water residence times.

The increase in pH levels is associated with more intense algae activity and CO_2 absorption in the process of photosynthesis. Besides, saline tidal intrusion of the Arabian Gulf leads to an increase in salinity and bicarbonate ion content in the water of the Shatt Al-Arab River.

Carbonate and bicarbonate ions are important regulators of water chemistry as their hydrolysis produces OH^- ions and hence increases the pH level. These ions are major buffer substances of aquatic systems because of the ability to resist rapid changes in pH. Therefore, carbonates and bicarbonates are considered to be among the most significant factors influencing alkalinity of surface and ground waters especially in regions with limestone deposits and those subjected to anthropogenic impact including irrigation, agricultural drainage, domestic sewage disposal, and other practices (Zhao et al., 2024).

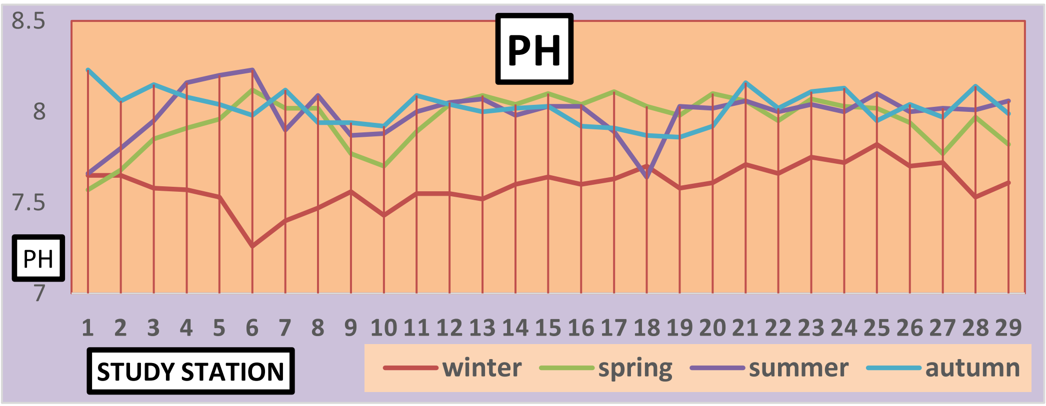

Figure 2. Seasonal Spatial Variation of pH Values in the Shatt Al-Arab River.

It is possible to note that there is a high chemical homogeneity in acid-base reactions along the Shatt Al-Arab River on the basis of the spatial distribution shown in figures 3 to 6. Variation in pH value in different sampling stations did not exceed 0.5 pH units. Such uniformity is due to dynamics of the river and constant mixing processes which allow water homogenization along the whole river course.

Figure 3 represents the data related to winter, when the minimum pH values were revealed; they vary from 7.26 to 7.60. Such low pH values are related to low water temperature, which favors CO2 dissolution and, consequently, formation of carbonic acid and decrease in pH value. Besides, during winter time biological activity of algae and other aquatic plants is reduced, that means that lower rate of CO2 consumption by photosynthesis occurs.

On the contrary, Figure 4 represents the data related to spring, where the increase of pH values was revealed (from 7.57 to 8.12). Such increase in pH values could be explained by increase of temperature and biological activity of organisms, especially of photosynthesizing ones which consume dissolved CO2 leading to reduction of carbonic acid concentrations and pH increase.

Maximum pH values were revealed during summer and autumn (Figures 5 and 6) and they vary from 7.66 to 8.23 and from 7.70 to 8.23, respectively. These maximum values of pH are caused by high temperature, evaporation and influence of saline tide from the Arabian Gulf. Gulf waters have higher content of carbonate and bicarbonate ions than the river water and, consequently, higher pH values and buffering capacity (Zhao et al., 2024).

Assessment of water suitability for irrigation by FAO criteria (FAO, 1985) shows that pH values in all sampling stations during the period of study fall into the recommended pH interval. However, only some stations have slightly increased pH values, but this increase was insignificant and does not influence water usability for agricultural irrigation.

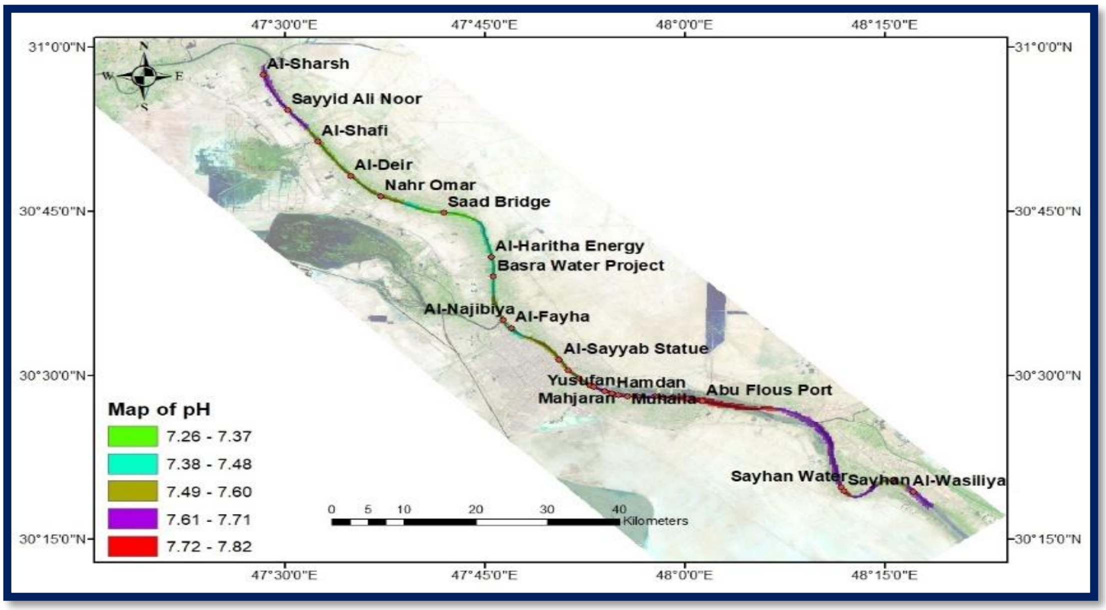

Figure 3. Spatial Distribution of pH Values in the Shatt Al-Arab River during Winter.

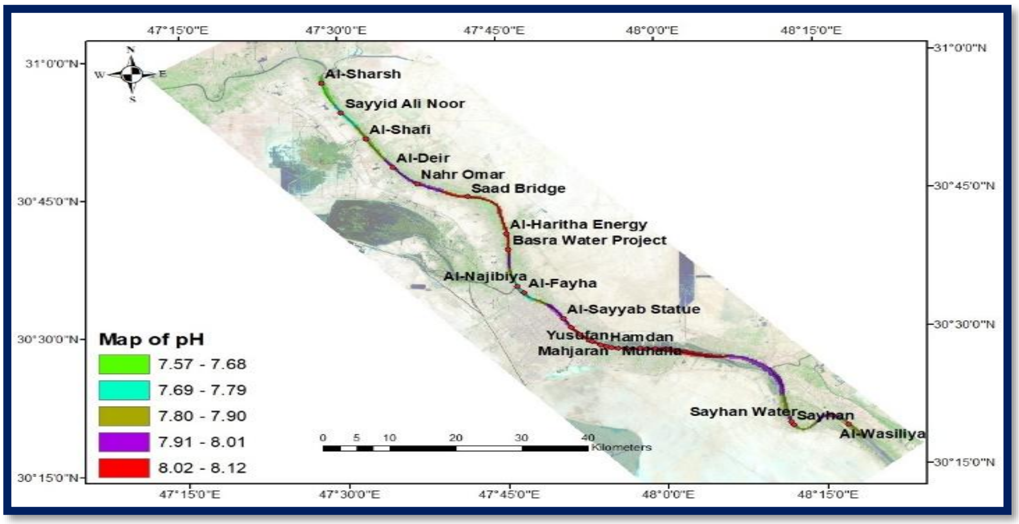

Figure 4. Spatial Distribution of pH in the Shatt Al-Arab River during Spring.

Natural Resources for Human Health
eISSN: 2583-1194

Figure 5. Spatial Distribution of pH in the Shatt Al-Arab River during Summer.

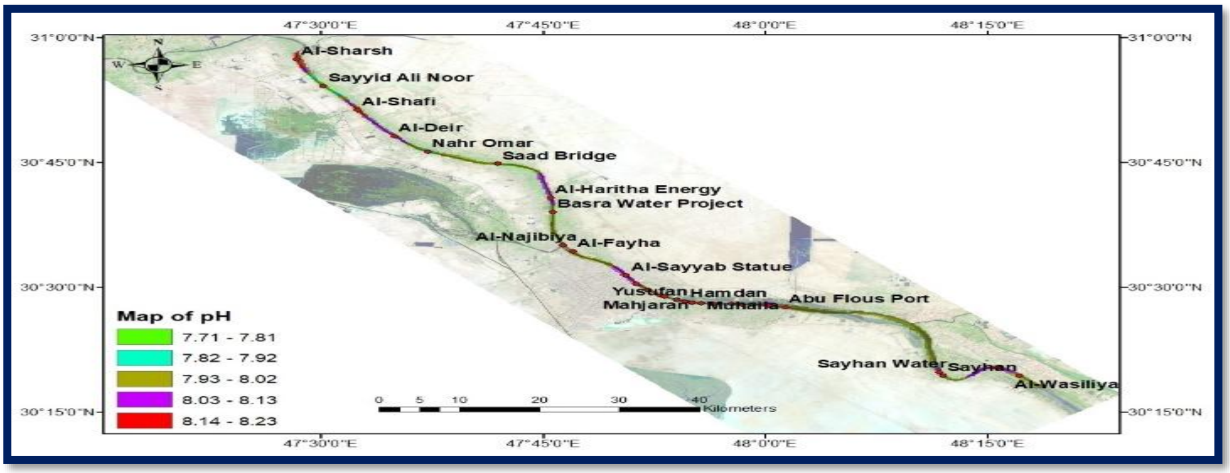

Figure 6. Spatial Distribution of pH in the Shatt Al-Arab River during Autumn**.**

Table 2. Monthly pH Values of the Studied Stations in the Shatt Al-Arab River

Stat	PH/	PH/	PH/	PH/	PH/	PH/	PH/	PH/	PH/	PH/	PH/	PH/	Aver
S1	7.91	7.83	7.77	7.36	7.77	7.33	7.61	7.73	7.78	7.48	8.25	8.53	7.78
S2	7.06	7.94	7.60	7.40	7.99	7.41	7.65	8.06	7.28	8.06	8.20	8.22	7.80
S3	7.56	7.85	7.64	7.25	7.88	7.70	7.97	8.36	7.40	8.10	8.50	8.40	7.88
S4	7.37	7.77	7.34	7.60	8.10	7.68	7.95	8.21	7.85	8.41	8.52	8.36	7.93
S5	7.38	7.94	7.12	7.53	7.83	7.87	8.18	8.54	7.73	8.33	8.36	8.39	7.93
S6	7.37	7.46	7.13	7.18	8.23	7.89	8.24	8.55	8.00	8.13	8.23	8.33	7.90
S7	7.85	7.73	7.19	7.28	7.73	8.05	8.27	8.25	8.05	7.39	8.14	8.36	7.86
S8	7.10	7.82	7.20	7.38	7.74	8.15	8.17	8.10	8.06	8.12	8.30	8.42	7.88
S9	7.52	7.66	7.60	7.41	7.94	7.67	7.69	8.15	7.86	7.59	8.04	8.25	7.78
S10	7.36	7.63	7.20	7.46	7.69	7.93	7.49	8.25	8.10	7.30	8.24	8.17	7.74
S11	7.90	7.72	7.40	7.52	8.10	7.78	7.80	8.18	7.98	7.85	8.12	8.26	7.88
S12	7.85	7.64	7.39	7.63	8.23	7.98	7.92	8.20	8.07	7.89	8.09	8.17	7.92
S13	7.59	7.68	7.66	7.23	8.14	7.97	8.16	8.08	8.00	8.13	8.14	8.26	7.92

S14	7.61	7.76	7.71	7.34	8.10	8.03	7.98	8.02	7.97	7.95	8.17	8.27	7.91
S15	7.63	7.64	7.76	7.53	8.22	8.05	8.03	8.01	7.96	8.13	8.20	8.26	7.95
S16	7.35	7.76	7.41	7.62	8.02	8.01	8.10	8.08	8.05	7.96	8.16	8.25	7.90
S17	7.38	7.75	7.62	7.51	8.20	8.08	8.04	8.16	8.12	7.40	8.07	8.29	7.89
S18	7.33	7.73	7.82	7.56	7.90	8.14	8.06	7.93	7.9	7.10	8.00	8.28	7.81
S19	7.00	7.62	7.44	7.68	8.05	8.08	7.80	8.02	7.90	8.17	8.25	8.32	7.86
S20	7.10	7.71	7.66	7.45	8.30	8.10	7.90	8.02	7.89	8.14	8.32	8.34	7.91
S21	7.02	7.70	7.73	7.70	8.05	8.12	8.00	8.04	7.92	8.21	8.43	8.43	8.00
S22	7.38	7.60	7.76	7.63	7.75	8.15	7.95	7.99	7.89	8.12	8.31	8.36	7.91
S23	7.58	7.66	7.80	7.80	8.08	8.11	8.02	8.02	7.94	8.17	8.28	8.48	8.00
S24	7.75	7.66	7.73	7.78	8.03	8.10	7.95	7.89	7.90	8.22	8.38	8.26	7.97
S25	7.12	7.77	7.84	7.85	8.10	8.06	7.89	7.97	8.04	8.28	8.32	8.42	7.97
S26	7.56	7.75	7.58	7.76	7.87	8.07	7.87	7.84	7.98	8.19	8.12	8.45	7.92
S27	7.35	7.72	7.60	7.84	7.27	8.01	8.03	7.88	8.00	8.19	8.15	8.41	7.87
S28	7.70	7.69	7.55	7.34	7.96	8.09	7.87	7.80	8.07	8.17	8.12	8.60	7.91
S29	7.45	7.66	7.60	7.56	7.70	7.86	7.91	7.85	8.03	8.30	8.12	8.39	7.87
Average	7.50	7.72	7.55	7.52	7.96	7.95	7.95	8.08	7.92	7.98	8.23	8.34	7.89

3. Electrical Conductivity (EC)

Monthly monitoring was conducted during a hydrological cycle of twelve months on the full stretch of the Shatt Al-Arab River, covering from the north to south of the river. It is observed in Table 3 below that there exists a longitudinal gradient of water salinity from the upper part where fresh to moderately saline water can be found to the south part where highly saline to marine water is encountered. The minimum EC of 2.0 dS m^{-1} was measured at Sayyid Ali Noor Station in November when the winter season starts. On the other hand, the maximum EC of 48.15 dS m^{-1} was measured at Al-Wasiliyah Port Station in September (autumn).

This indicates that there exists a wide range of variation in the electrical conductivity, which indicates the transition of EC values from slightly saline water in the north of the river to highly saline water in the south of the river. At certain times of the year, the EC values of the southern stations exceed the values of seawater. This is caused by saline water intrusion into the river from the Arabian Gulf due to tides and effluents such as municipal wastewater, which contains high concentration of dissolved salt. In addition, the reduced amounts of freshwater entering from the four tributaries of the Shatt Al-Arab including Tigris, Euphrates, Karkheh, and Karun rivers have contributed to the increased salinity levels in the river.

In line with above findings, previous studies also observed an increasing trend in EC values in moving towards the estuary region of the Shatt Al-Arab River (Al-Bazouni, 2023). Likewise, according to Al-Asadi & Al-Lami (2014), the highest EC values occur close to the river mouth due to tidal effects while EC decreases significantly upstream due to tidal effects reduction and dilution of freshwater coming from the Tigris River.

4. Spatial Distribution of Electrical Conductivity During the Seasons

Seasonal variations in electrical conductivity (EC) at stations under investigation are shown in Figure 7. It should be noted that in the investigated seasons, EC was the main factor responsible for determining water quality. Significant changes in the seasonal dynamics of water quality were observed, since the highest EC values were registered in summer, while the lowest ones – in winter.

So, in summer the maximum values of EC were observed in the southern stations: Saihan Water Project, Saihan, Al-Siba and Al-Wasiliyah with the values of 38.60-47.00 dS m^{-1}. The lowest EC values were revealed at the northern stations: Al-Sharash, Sayyid Ali Noor, Al-Shafi, Al-Dair, Nahran Omar and Saad Bridge with the values of 3.24-13.04 dS m^{-1}. An increase in the salinity at southern stations reached about 260% compared to the northern stations.

In spring and autumn, the same tendency to have higher EC values at the southern stations was observed. In spring, the values of EC ranged from 16.52 to 22.23 dS m^{-1}, whereas in autumn – 31.20-33.90 dS m^{-1}. In contrast to southern stations, the lowest

EC values were registered in the northern stations: Al-Sharash, Sayyid Ali Noor, Al-Shafi, Al-Dair, Nahran Omar, Saad Bridge, Al-Hartha (Power Station) and Basrah Water Project. The values were 3.38-6.44 dS m⁻¹ in spring with approximately 245% increase at southern stations. In autumn the values of EC in the northern stations were 3.93-15.40 dS m⁻¹ with approximately 120% increase in the southern sector.

The lowest EC values among all seasons were found in winter. Northern stations (Al-Sharash, Sayyid Ali Noor, Al-Shafi, Al-Dair, Nahran Omar, and Saad Bridge) had the values of 2.57-4.13 dS m⁻¹. At the same time, the highest values of EC in winter were detected at Al-Siba and Al-Wasiliyah with values of 8.35 and 7.56 dS m⁻¹, respectively.

It is worth mentioning that the spatial distribution maps (Figures 8-11) demonstrate the evident spatio-temporal variations in EC values and their dominating role in shaping the water quality of the Shatt Al-Arab River. So, in winter and spring (Figures 8 and 9), about 20.7% of sampling stations, located mainly in the northern sector, belonged to the water suitable for irrigation of certain salt-sensitive crops and all moderately salt-tolerant crops. In contrast to it, in summer and autumn (Figures 10 and 11), the majority of stations in the central part of the river (about 65.5% of the study area) were considered as the water suitable only for moderately salt-tolerant and salt-tolerant crops. Southern stations, comprising approximately 13.8% of sampling stations, were not appropriate for irrigation and could be used only for highly salt-tolerant crops.

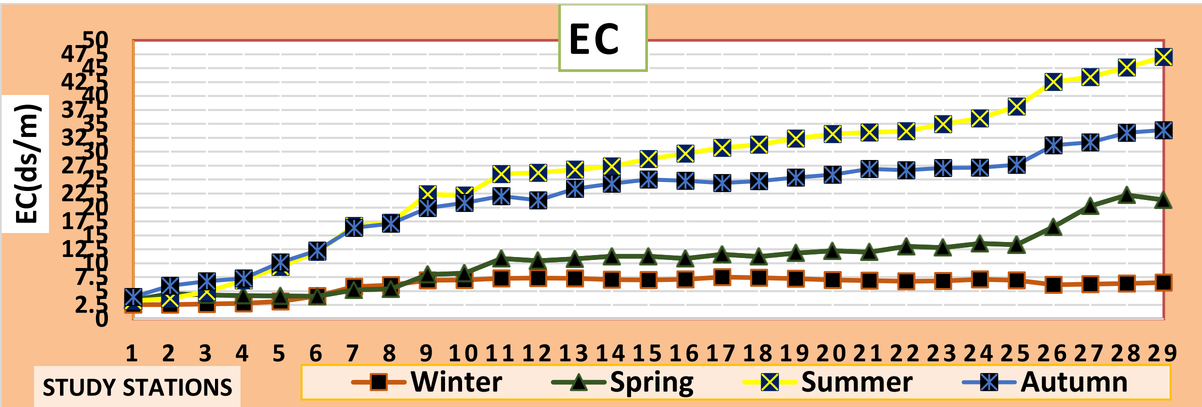

Figure 7. Electrical Conductivity (EC) Values (dS m⁻¹) at the Studied Stations during the Four Seasons.

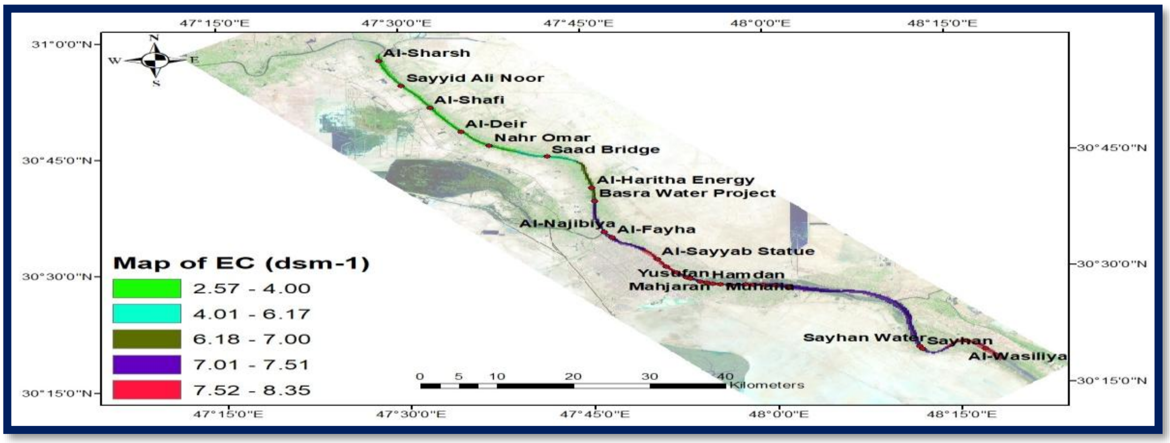

Figure 8. Spatial Distribution of Electrical Conductivity (EC) in the Shatt Al-Arab River during Winter

Natural Resources for
Human Health
eISSN: 2583-1194

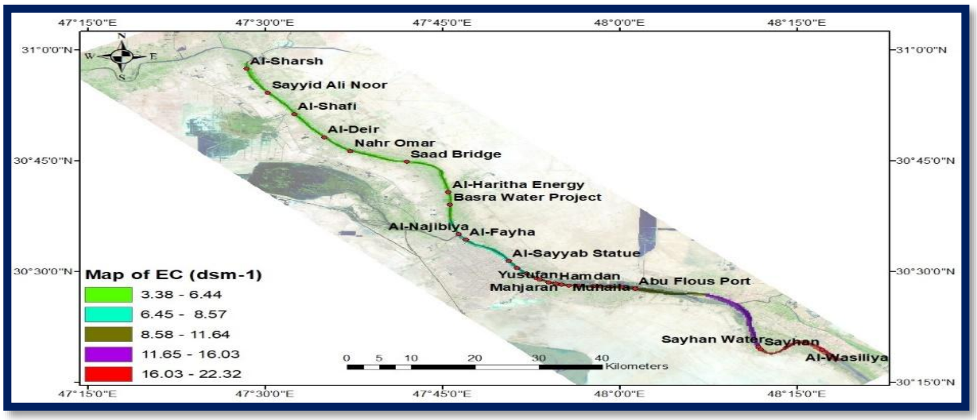

Figure 9. Spatial Distribution of Electrical Conductivity (EC) in the Shatt Al-Arab River during Spring.

Table 3. Monthly Electrical Conductivity Values (dS m⁻¹) at the Studied Stations along the Shatt Al-Arab River

Sta	E C/	E C/	EC/	EC/	EC/	EC/	EC/	EC/	EC/	EC/	EC/	EC/	Aver
S1	2.18	2.21	2.53	2.98	4.02	2.76	3.37	2.97	2.84	3.91	3.28	6.34	3.28
S2	2.00	2.31	2.57	2.91	4.90	5.45	3.20	3.14	2.89	5.00	4.98	10.95	4.19
S3	3.50	2.57	2.59	2.83	4.45	5.34	3.10	3.50	4.68	6.50	4.49	12.29	4.65
S4	2.70	2.84	2.66	2.84	4.13	5.29	3.11	3.53	8.71	8.65	4.95	14.24	5.30
S5	2.20	3.62	2.75	3.11	3.96	5.58	2.82	5.00	12.50	10.47	12.21	16.10	6.69
S6	2.90	4.78	3.26	4.36	4.00	5.44	2.84	7.60	13.30	13.6	15.74	18.25	8.01
S7	5.10	5.71	5.55	6.05	5.93	6.88	2.90	12.30	14.20	18.80	21.65	22.30	10.61
S8	5.24	5.48	6.16	6.50	6.54	6.79	2.83	12.16	16.50	19.10	22.70	23.30	11.11
S9	5.50	5.83	8.13	6.86	6.76	7.33	9.80	17.60	22.70	26.50	24.74	29.50	14.27
S10	6.32	6.18	7.75	7.00	6.95	7.42	10.18	18.10	23.80	24.50	24.00	32.10	14.53
S11	5.40	6.62	7.63	7.66	7.56	7.19	17.80	21.30	26.50	30.30	27.56	33.20	16.56
S12	5.81	6.85	7.50	7.66	7.78	7.34	16.16	21.70	26.90	30.10	28.32	29.80	16.33
S13	6.76	6.25	7.72	7.80	7.85	8.10	16.34	22.40	26.70	31.40	29.75	33.50	17.05
S14	6.80	6.10	7.71	7.43	8.02	7.92	17.75	23.75	27.30	30.90	32.27	33.80	17.48
S15	7.68	5.58	7.65	7.74	7.99	7.70	18.08	25.61	28.10	32.40	33.46	33.90	17.99
S16	7.10	5.98	7.54	7.80	7.98	7.95	16.65	27.30	29.40	32.40	33.57	33.70	18.11
S17	7.12	7.13	7.63	7.76	7.92	8.15	18.72	28.70	31.20	32.20	32.90	33.20	18.55
S18	70	6.88	7.47	7.85	7.88	8.22	17.43	28.50	32.90	32.40	33.35	33.80	18.64
S19	7.20	6.37	7.44	7.83	7.86	8.39	19.16	29.10	33.30	34.80	34.14	34.8	19.20
S20	6.70	5.82	7.45	7.65	7.75	8.61	20.30	29.10	33.60	36.90	35.30	35.60	19.57
S21	7.35	5.76	7.41	7.52	7.67	9.10	19.15	29.80	33.30	37.30	36.70	36.70	19.81
S22	6.82	5.77	7.23	7.38	7.62	9.14	22.40	28.50	34.70	37.90	37.45	35.90	20.07
S23	7.14	5.85	7.31	7.32	7.57	9.45	21.30	30.50	36.30	38.10	38.34	35.80	20.42
S24	7.76	6.88	7.20	7.27	7.53	9.73	23.30	31.30	37.40	38.30	38.53	35.20	20.87
S25	7.25	6.50	7.13	7.25	7.48	9.91	22.60	32.10	40.20	38.40	39.48	36.30	21.22
S26	6.76	5.02	5.75	7.65	8.41	8.86	32.30	42.30	43.90	41.40	44.23	42.60	24.10
S27	6.65	5.57	5.66	7.45	10.90	11.74	38.20	43.40	45.10	41.80	44.91	43.5	25.41
S28	7.30	7.56	8.76	8.73	14.00	14.68	38.10	44.60	46.40	43.40	46.37	46.60	27.21
S29	6.74	5.88	7.25	9.55	13.40	13.76	38.90	46.45	47.20	47.66	48.15	46.80	27.65
Aver	5.83	5.51	6.32	6.65	7.41	8.08	16.51	23.18	26.98	28.45	28.74	30.35	16.17

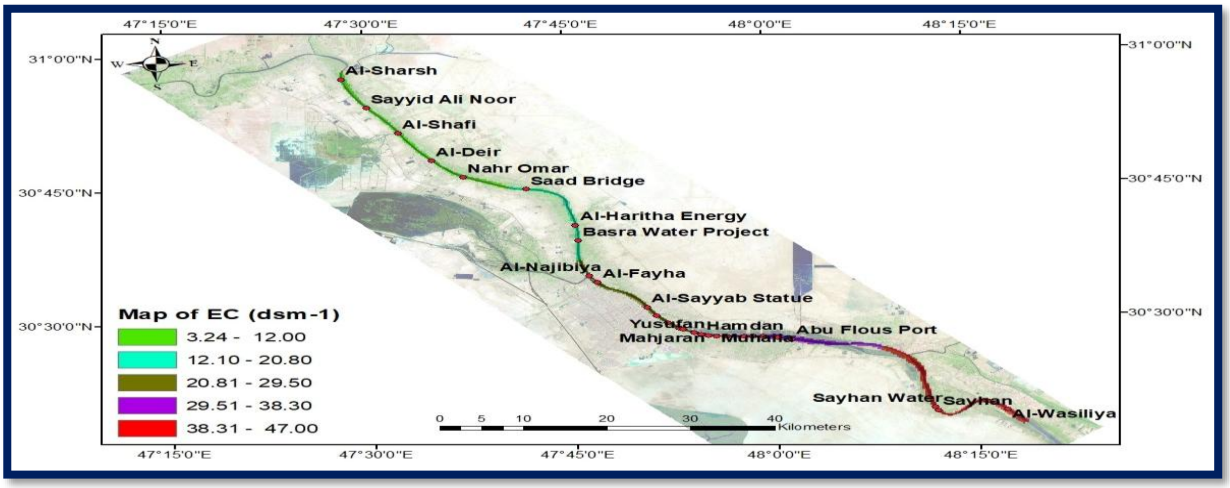

Figure 10. Spatial Distribution of Electrical Conductivity (EC) in the Shatt Al-Arab River during Summer

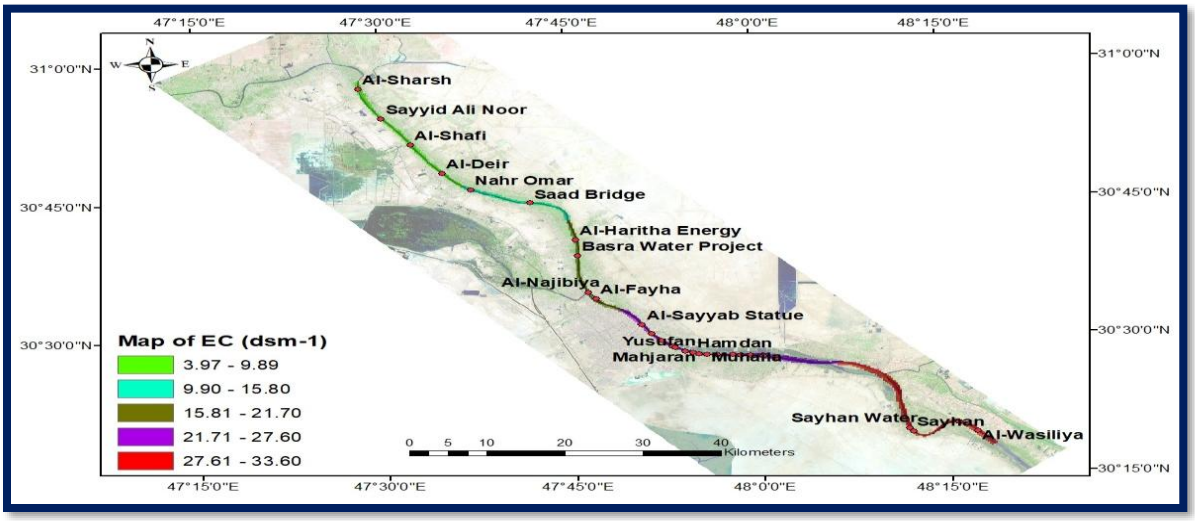

Figure 11. Spatial Distribution of Electrical Conductivity (EC) in the Shatt Al-Arab River during Autumn.

5. Total Dissolved Solids (TDS)

Results presented in Table 4 have shown that there are significant gradients both in space and time for the concentration of total dissolved solids (TDS) in the Shatt Al-Arab River as a consequence of the influence of hydrometeorological and marine factors. The lowest TDS concentration is 1,000 mg L^{-1} in Sayyid Ali Noor Station, while the second lowest is 1,100 mg L^{-1} in Nahran Omar Station, which occurs in November. Low values of TDS are the consequence of the decreased rate of evaporation caused by low temperatures, small amount of saline tidal intrusion, and also the dilution process with freshwaters from the Tigris River. Also, the amount of wastewater discharges in this area is relatively low since this area is distant from urban areas.

The highest TDS concentration is 32,800 mg L^{-1} in August (summer) in Al-Wasiliyah Port Station. This increased value means that the gradual change of water from freshwater towards brackish and then saline water takes place. This type of conditions is associated with the intrusion of seawater from the Arabian Gulf, small amount of freshwater discharge from the Tigris River, the main source of freshwater in the Shatt Al-Arab River, and high temperatures increasing the evaporation. Furthermore, the increased discharges of wastewater to the southern part of the river contribute to high dissolved salt concentrations. Results are in agreement with the findings of Al-Eidawi (2021) and Al-Bazouni (2023).

6. Spatial Distribution of Total Dissolved Solids (TDS) During the Seasons

It is evident from Figure 12 that there exist obvious seasonal changes of total dissolved solids (TDS) concentration, whereby the lowest concentrations usually occur during the high river discharge period (for example, rainy season and water release periods). This is as a result of dilution effect. On the other hand, the highest TDS concentrations occur during summer period since the evaporation rate increases and hence river discharge decreases with increased saline intrusion.

The seasonal changes in TDS concentration are very high at the southern stations than the northern stations. In summer, the highest concentrations, which vary from 27,467 to 31,567 mg L^{-1} occurred at the southern stations (Saihan Water Project, Saihan, Al-Siba, and Al-Wasiliyah Port). Central stations from Al-Hartha Power Station to Abu Flous Port, which constitute 62% of the sampling stations recorded concentrations varying from 6,967 to 22,467 mg L^{-1}. On the other hand, the lowest concentrations varied from 1,433 to 4,833 mg L^{-1} at the northern stations.

Increased concentrations during summer period occur due to the high temperature, high evaporation rate, saline tidal intrusion and increased use of the water for domestic, agriculture and industrial uses. With regard to the central stations, the TDS concentrations at the southern stations increased by 40.5%. However, at the northern stations, the increase in concentrations was 553% with respect to the central stations.

Winter season experiences the lowest TDS concentrations since the temperature is low, precipitation is high, evaporation rates are low and consequently the dilution of dissolved salts is high. During winter, TDS concentrations at the southern stations varied from 2,567 to 3,633 mg L^{-1}, while at the northern stations, the concentrations varied from 1,267 to 1,800 mg L^{-1}, which represent an increase of approximately 101.8%.

During autumn and spring periods, the southern stations still experience the highest concentrations, which vary from 19,600 to 22,033 mg L^{-1} and from 8,733 to 12,367 mg L^{-1}, respectively. At the northern stations, TDS concentrations vary from 1,767 to 5,833 mg L^{-1} during autumn, and from 1,533 to 1,933 mg L^{-1} during spring. The percentage increase in the TDS concentration at the southern stations reached approximately 277.7% during autumn and 553% during spring.

These results agree with those obtained by Al-Silawy et al. (2025), where the highest TDS concentration occurred at Al-Faw station during summer period (27,045 mg L^{-1}) and the lowest occurred at Al-Qurnah station during winter (9,965 mg L^{-1}).

Figures 13–16 illustrate the seasonal distribution of TDS concentration at all sampling stations. From the results, there exists a gradient of concentrations along the continuum of the river. The northern stations (S1–S6) record the lowest concentrations, which range from 1,504 to 3,567 mg L^{-1}. There is gradual increase in the concentrations at the central stations (S7–S15), where the concentration ranges from 5,000 to 9,550 mg L^{-1}. In addition, at the southern stations (S16–S29), there is sharp increase in the concentrations, where some of the stations record concentrations higher than 10,000 mg L^{-1}, thus representing the transition from the freshwater to brackish and saline waters (Brackish–Saline System).

The above spatial pattern results from increased intrusion of saline water due to increased marine tide towards the Arabian Gulf region. Furthermore, the decreased inflow of the fresh water due to reduction in the discharge of the rivers reduces the river diluting capacity. Besides, the high evaporation rates associated with the hot climate of the region contribute to high concentrations. Also, increased pollution sources from agricultural drainage, industrial wastewater and domestic sewage contribute to increased ionic loads and consequently TDS concentrations.

During winter (Figure 13), approximately 24% of the sampling stations, which are located mainly in the northern sector, recorded TDS concentrations between 1,270 and 2,000 mg L^{-1}. The rest 76% of the study area from Al-Hartha Power Station to Al-Wasiliyah Port recorded concentrations between 2,001 and 3,300 mg L^{-1}.

During spring (Figure 14), the concentrations range from 1,530 to 3,700 mg L^{-1} in the northern stations and parts of the central stations (approximately 34.5% of sampling locations). The remaining stations recorded higher concentrations ranging from 3,701 to 12,700 mg L^{-1}.

Autumn (Figure 15) experienced northern stations TDS values between 1,770 and 5,750 mg L^{-1}. Meanwhile, the central and southern stations, which consist of about 76% of the study area, recorded 5,751–21,700 mg L^{-1}.

Natural Resources for Human Health
eISSN: 2583-1194

Summer (Figure 16) records the highest TDS concentrations among all seasons since the evaporation rates increase due to high temperatures, while the river discharge is decreased and water consumption and saline intrusion are increased. In this case, the northern stations have 1,430–7,460 mg L^{-1}, while central and southern stations exhibit higher concentrations of 7,461 to 31,600 mg L^{-1}.

Based on the United States Salinity Laboratory classification according to Richards (1954), the majority of the sampling stations in all the four seasons are characterized by the "Very High Salinity", except the first four northern stations in winter, which are categorized under "High Salinity" water.

According to the FAO (1985) classifications, the northern stations (20.7% of the studied locations) were categorized as low-to-moderate salinity in winter and spring seasons. On the other hand, the central and southern stations were categorized as highly saline. In summer and autumn, all sampling stations belonged to the highly saline category.

Based on the recorded TDS concentrations, the sampling stations can be classified as follows:

1. **Stations S1–S5:** Freshwater to slightly saline water.
2. **Stations S6–S15:** Brackish water.
3. **Stations S16–S29:** Saline to highly saline water.

This classification is consistent with internationally recognized water-quality standards and reflects the progressive salinization of the Shatt Al-Arab River toward its estuarine zone.

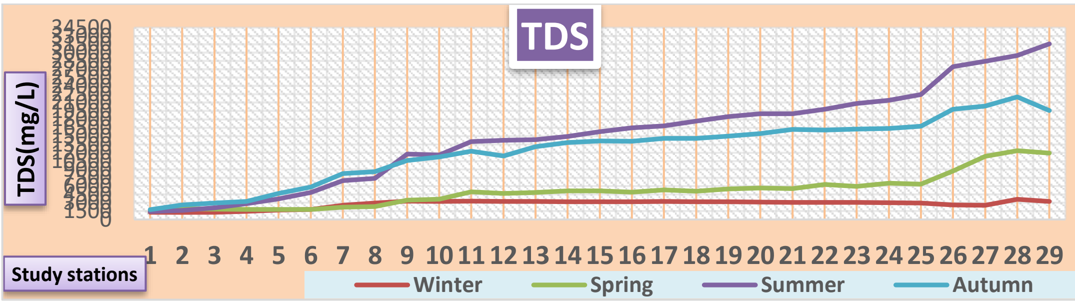

Figure 12. Seasonal Variation of Total Dissolved Solids (TDS) in the Shatt Al-Arab River.

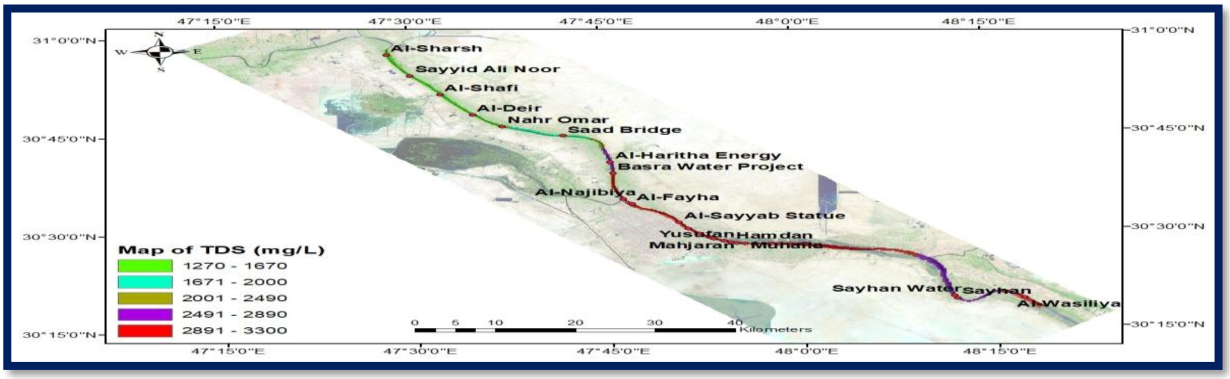

Figure 13. Spatial Distribution of Total Dissolved Solids (TDS) in the Shatt Al-Arab River during Winter.

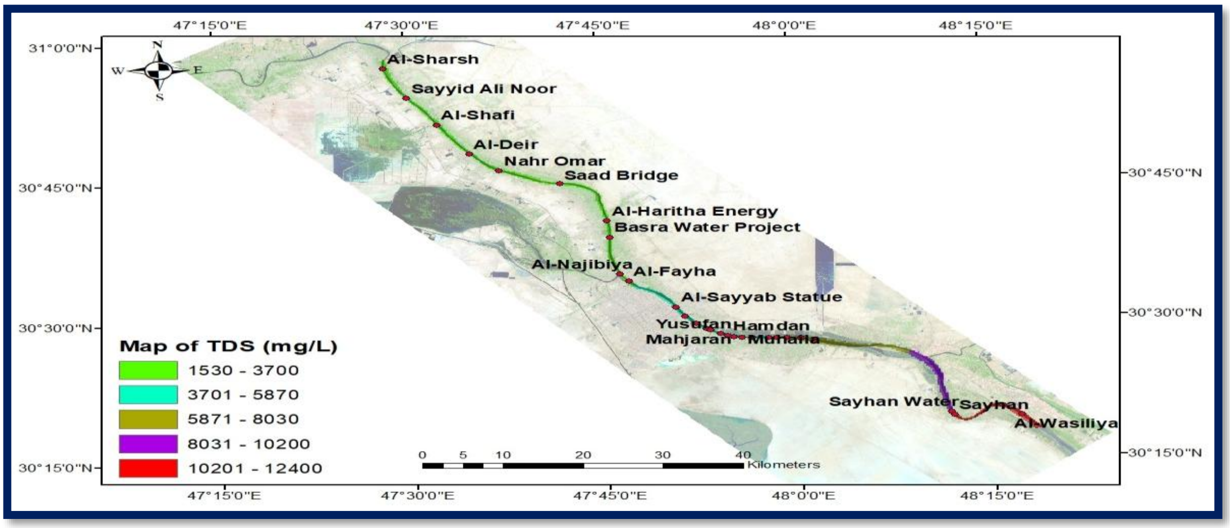

Figure 14. Spatial Distribution of Total Dissolved Solids (TDS) in the Shatt Al-Arab River during Spring.

Figure 15. Spatial Distribution of Total Dissolved Solids (TDS) in the Shatt Al-Arab River during Autumn.

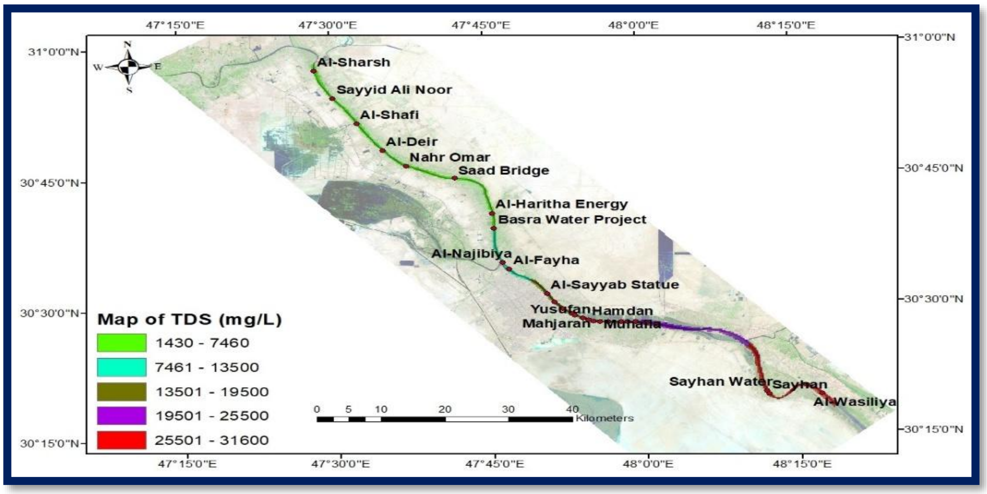

Figure 16. Spatial Distribution of Total Dissolved Solids (TDS) in the Shatt Al-Arab River during Summer.

Table 4. Monthly (TDS) Concentrations (mg L⁻¹) at the Studied Stations along the Shatt Al-Arab River.

Stat	TDS	TDS	TDS	TDS	TDS	TDS	TDS	TDS	TDS	TDS	TDS	TDS	Ave
S1	1200	1250	1200	1400	1800	1300	1500	1400	1200	1700	1400	2700	1504
S2	1000	1300	1200	1300	2100	2300	1400	1400	1300	2200	2100	4800	1867
S3	1500	1400	1200	1300	1900	2300	1400	1500	2000	2700	1900	5500	2050
S4	1200	1800	1300	1300	1800	2300	1400	1500	3400	3700	2100	6500	2358
S5	1100	2300	1300	1400	1700	2400	1300	2200	4200	4700	5400	7600	2967
S6	1400	2000	1500	1900	1800	2300	1300	3300	5000	6200	7300	8800	3567
S7	2200	2600	2400	2600	2500	2900	1300	5200	6500	9200	10900	11700	5000
S8	2200	3400	2600	2800	2800	2900	1300	5100	7800	9300	11600	12000	5317
S9	2400	3500	3500	2900	2900	3100	4500	8500	12400	14300	13000	16500	7292
S10	2700	3500	3300	3000	3000	3100	4900	8800	12900	13000	12500	18600	7442
S11	2300	3300	3300	3300	3200	3100	8600	10700	14300	17000	15000	19500	8633
S12	2600	3200	3200	3300	3300	3100	7600	11100	14600	17000	14800	16800	8383
S13	2900	3100	3300	3400	3400	3500	7700	11500	14400	17200	16700	19700	8900
S14	2900	3000	3300	3200	3500	3400	8500	12400	14800	17600	18600	20000	9267
S15	3300	2900	3300	3300	3400	3300	8700	13200	15300	18800	19100	20000	9550
S16	3000	3000	3200	3300	3400	3400	7900	14800	16000	18700	19300	19900	9658
S17	4100	3100	3300	3300	3400	3500	9100	14900	17100	18500	19800	19900	10000
S18	3000	2900	3200	3400	3400	3500	8300	15200	19100	18800	20800	20000	10133
S19	3100	2900	3200	3400	3400	3600	9400	15100	19500	20800	21200	20700	10525
S20	3000	2900	3200	3300	3300	3700	10000	15100	19600	22300	21900	21500	10817
S21	3200	2900	3200	3200	3300	3900	9400	14900	19500	22600	23400	22000	10958
S22	2900	2900	3100	3200	3300	4000	11500	15200	20800	23500	23700	21700	11317
S23	3100	2900	3100	3200	3200	4100	10600	17000	21900	23600	24000	21600	11525
S24	3400	2900	3100	3100	3200	4200	12100	17500	23100	23700	24500	21200	11833
S25	3100	2800	3000	3100	3200	4300	11600	18600	24900	23900	25300	21900	12142
S26	2800	2200	2500	3200	3600	3800	18800	27400	28300	26700	29300	27400	14667
S27	2400	2100	2400	3200	4800	5400	23900	28900	29300	27100	30100	28700	15692
S28	3400	3300	3800	3800	6600	6800	23700	29400	30100	28900	31100	31600	16875
S29	3000	2500	3100	4200	5500	5900	24400	31600	30300	32800	24000	31800	16592
Aver	2566	2684	2734	2872	3197	3497	8693	12876	15503	16776	16924	17952	8865

7. Turbidity (TUR)

The results shown in Table 5 and Figure 17 show marked variations in the turbidity levels of Shatt Al-Arab River. The results showed spatial variation in turbidity levels with the stations closer to the estuarine area having the highest levels. The Saihan, Al-Siba, and Al-Wasiliyah are the stations with the highest turbidity levels where the highest level recorded was 173 NTU at Al-Siba station while 167 NTU at Saihan station in May and August. The increase in turbidity levels in this part of the river is due to the effects of the tide in resuspending bottom and bank sediments thus increasing the amount of suspended matter in the water body. Some other contributors include boat/ship activities and low flow of the river.

As seen in Figure 18, the lowest turbidity levels were recorded during autumn. Summer had the highest turbidity levels compared to other seasons as shown in Figure 21. This increase in turbidity levels during summer is due to increased human activities and decreased river flow in addition to the effects of the tide. The turbidity levels in southern stations were from 113 to 134 NTU while those of central and northern stations were from 27.6 to 91.6 NTU.

Relationships between Water Quality Parameters (pH, TDS, and Turbidity)

The interpretation of the results shows that there is a number of interdependencies between the parameters considered:

Firstly, there is an evident positive correlation between TDS and pH. In the southern stations, during summer and autumn there was an increase in TDS values and a corresponding shift to higher pH values. Such a trend can be caused by a higher concentration of ions dissolved in water, especially bicarbonates, which result from the mixture of seawater intrusion and river water. The higher concentration of such ions increases the ability of water to buffer, making the pH more alkaline.

Secondly, the correlation between TDS and turbidity is not always proportional. At times, a higher value of TDS is not accompanied by a higher turbidity, which means that dissolved and suspended solids are controlled by different environmental processes.

Thirdly, the positive correlation between turbidity and pH values was registered. Higher values of turbidity were followed by the increase in pH values. Such a trend can be caused by the impact of alkaline ions which enter the water as a result of saline water intrusion and lead to increased turbidity.

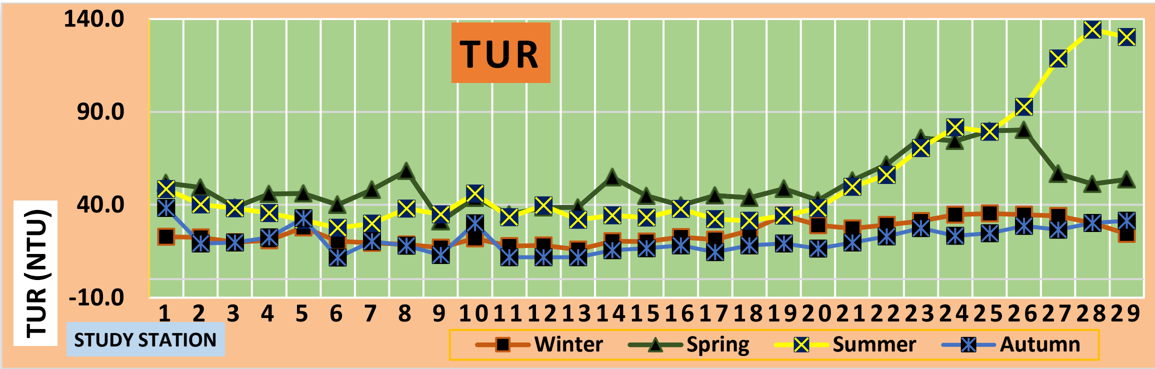

Figure 17. Turbidity (NTU) Values at the Studied Sampling Stations in the Shatt Al-Arab River.

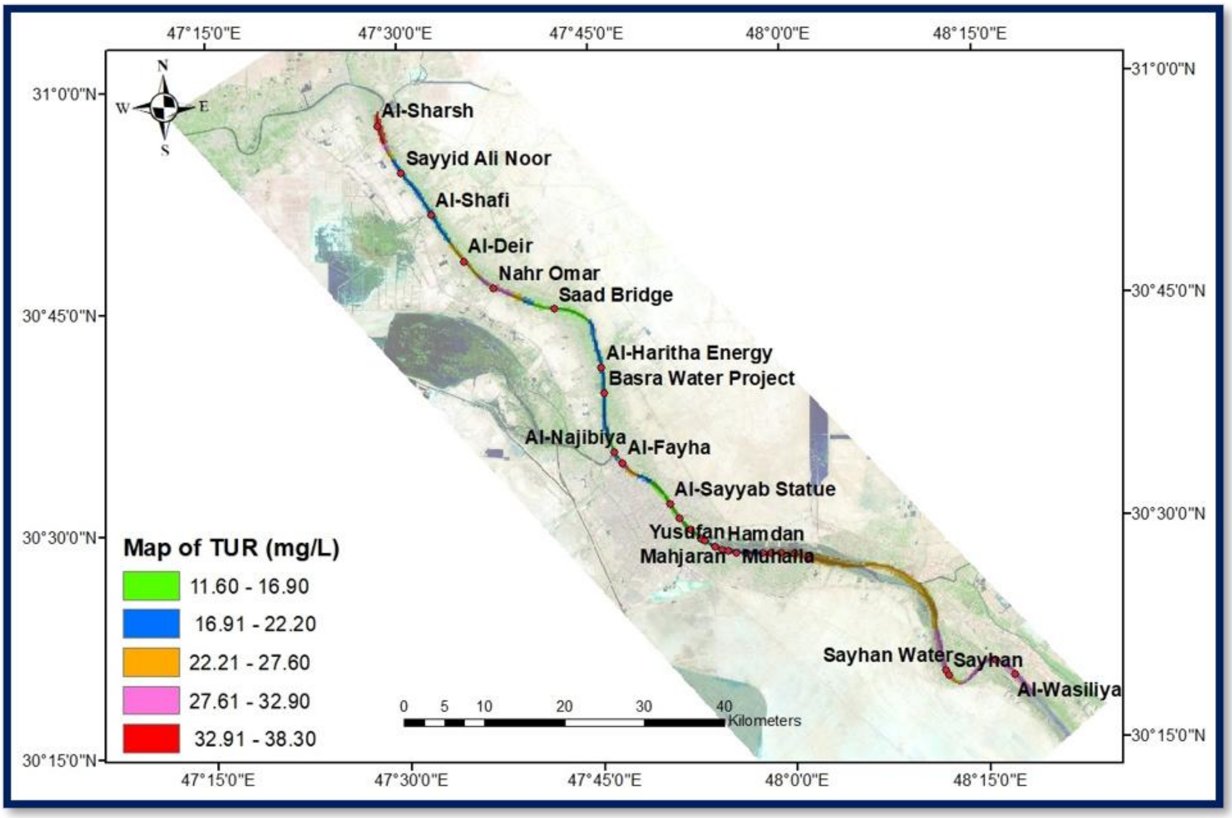

Figure 18. Spatial Distribution of Turbidity (NTU) in the Shatt Al-Arab River during Autumn.

Natural Resources for
Human Health
eISSN: 2583-1194

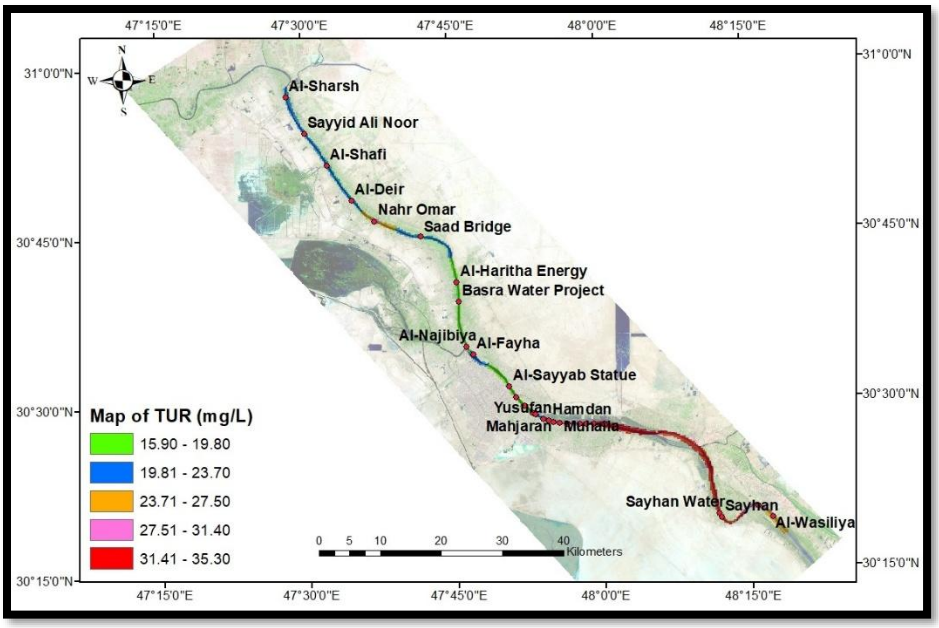

Figure 19. Spatial Distribution of Turbidity (NTU) in the Shatt Al-Arab River during Winter.

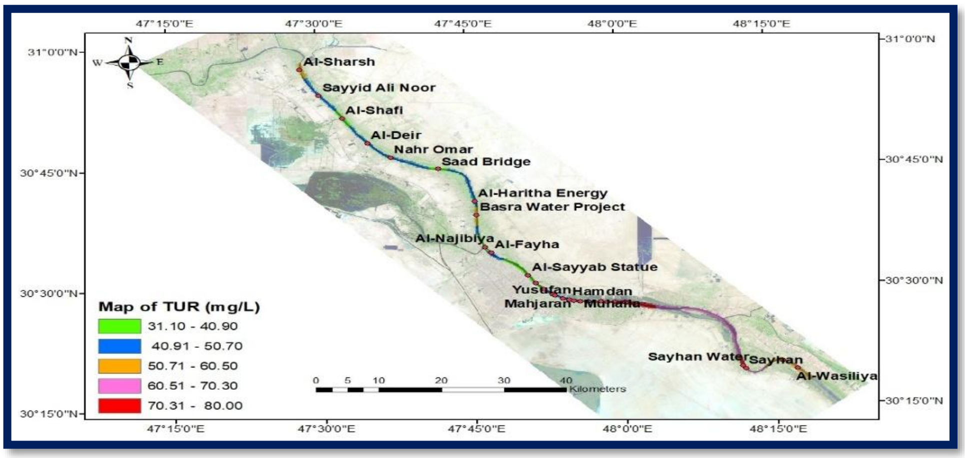

Figure 20. Spatial Distribution of Turbidity (NTU) in the Shatt Al-Arab River during Spring.

Table 5. Monthly Turbidity (NTU) Values at the Studied Stations along the Shatt Al-Arab River.

Sta	TUR1	TUR1	TUR	TUR	TUR	TUR	TUR	TUR	TUR	TUR	TUR	TUR	Ave
S1	12.5	22.1	18.5	27.9	27.5	50.1	77.5	70.0	36.8	38.5	38.2	64.1	40.3
S2	11.7	21.1	20.5	25.8	24.3	4.06	77.6	65.0	31.5	23.9	24.5	21.5	32.8
S3	14.2	19.8	17.7	21.9	25.0	38.0	53.0	52.0	22.4	39.8	22.7	22.2	29.1
S4	16.1	22.6	23.0	17.0	24.5	52.1	60.9	49.3	24.7	32.7	39.5	11.8	31.2
S5	14.6	29.2	27.0	27.3	29.0	49.0	60.4	43.0	21.9	30.3	60.8	22.8	34.6
S6	13.2	16.9	19.5	24.6	26.7	44.0	49.6	47.0	24.0	11.7	13.1	8.37	24.9
S7	15.0	15.9	24.0	18.8	27.8	61.0	55.6	47.8	26.7	15.3	28.6	17.7	29.5
S8	16.3	11.5	22.0	22.4	34.2	50.0	90.5	53.4	36.8	23.8	22.3	15.5	33.2
S9	17.8	14.1	16.0	20.6	27.0	28.5	37.7	51.7	33.2	19.7	8.1	13.2	24.0
S10	21.5	12.8	17.0	36.0	25.7	30.0	75.6	64.3	45.6	28.4	41.4	27.2	35.5

Natural Resources for
Human Health
eISSN: 2583-1194

S11	13.7	10.8	15.4	27.3	25.8	33.0	45.8	52.7	29.7	17.6	8.9	12.9	24.5
S12	17.5	11.4	20.0	23.0	28.3	47.3	39.6	63.6	35.4	19.9	5.3	12.7	27.0
S13	16.7	9.1	18.5	20.0	26.2	40.1	49.8	49.7	28.7	17.5	11.6	7.1	24.6
S14	16.5	8.6	19,6	33.2	41.8	47.5	75.3	52.2	27.6	23.0	16.5	13.6	32.3
S15	21.0	28.7	15.2	17.0	27.0	37.0	70.6	49.8	32.5	17.3	18.4	10.4	28.7
S16	9.66	20.2	25.5	22.0	27.0	32.0	60.2	47.5	37.2	28.6	33.1	11.7	29.6
S17	10.7	13.9	27.4	22.5	34.0	33.0	67.9	43.7	29.6	23.4	26.2	6.7	28.3
S18	14.2	24.6	29.5	24.0	28.0	35.0	68.4	39.7	28.2	26.2	29.4	11.1	29.9
S19	13.8	39.8	37.0	26.0	32.0	41.5	72.7	49.8	31.4	21.5	19.8	23.9	34.1
S20	12.2	30.6	29.3	27.0	25.4	30.0	71.8	55.7	40.3	18.5	22.3	14.7	31.5
S21	15.2	22.0	29.9	30.0	27.7	61.3	70.6	61.8	54.4	32.7	28.7	15.2	37.5
S22	20.5	30.5	26.0	31.0	35.6	59.5	90.2	71.6	59.8	36.8	31.6	16.9	42.5
S23	21.0	33.9	37.0	23.0	39.0	79.2	110.0	100.0	86.4	25.3	27.4	33.9	51.3
S24	29.0	40.0	32.0	32.0	37.0	71.2	115.0	110.0	106.0	29.4	23.5	17.4	53.5
S25	15.2	38.9	33.0	34.0	35.7	92.0	112.0	108.0	101.0	28.9	29.6	29.2	54.8
S26	31.7	37.0	31.0	36.0	49.8	70.0	121.0	120.0	87.4	71.0	23.5	30.8	59.1
S27	16.6	30.0	35.0	37.0	28.5	58.0	84.0	150.0	98.4	108.0	29.9	33.4	59.1
S28	22.0	38.0	18.7	34.0	37.5	51.2	65.0	117.0	110.0	173.0	39.1	29.6	61.3
S29	21.0	21.0	17.7	34.5	36.0	66.0	59.0	167.0	112.0	116.0	41.3	31.7	60.3
aver	16.9	23.3	24.4	26.8	30.8	49.4	72.0	70.8	49.6	37.9	26.4	20.3	37.4

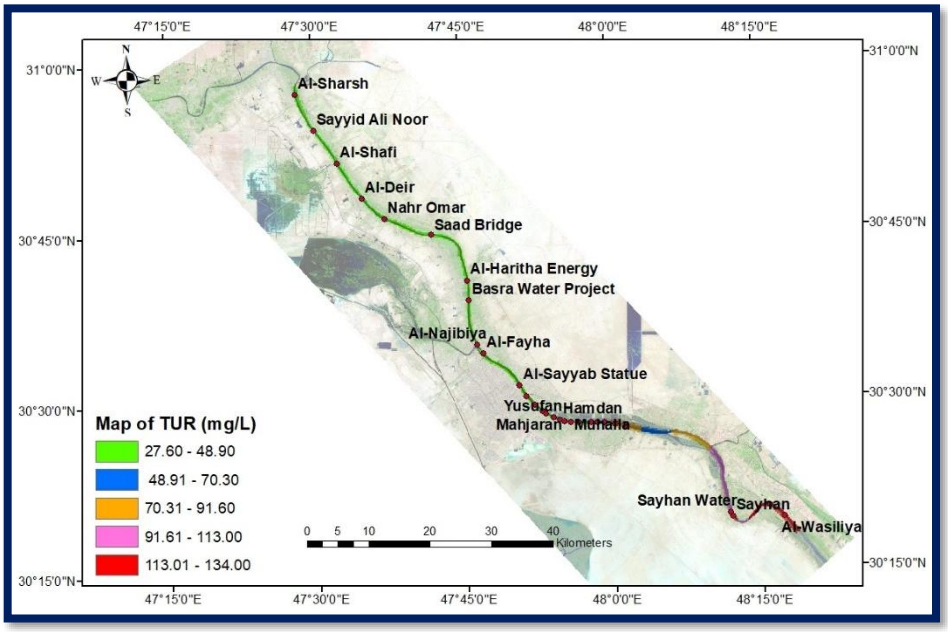

Figure 21. Spatial Distribution of Turbidity (NTU) in the Shatt Al-Arab River during Summer

CONCLUSIONS

- This study demonstrated that the integration of Geographic Information Systems (GIS) and Remote Sensing (RS) is a powerful and effective tool for monitoring and analyzing the spatial and temporal distribution of water quality in the Shatt Al-Arab River.

- The results revealed a clear deterioration in water quality toward the estuarine zone, particularly in terms of salinity and turbidity. A distinct seasonal effect was also observed, with more severe conditions occurring during summer and autumn.

RECOMMENDATIONS

1. The establishment of a sustainable environmental monitoring system based on Remote Sensing (RS) and Geographic Information Systems (GIS) is recommended for the effective management of water quality in the Shatt Al-Arab River.
2. Water resource management should be improved by increasing freshwater inflows from the Tigris and Euphrates Rivers and reducing uncontrolled water usage along the river system.

REFERENCES

[1] A l-Amiri, N. J., & Disher, M. A. (2021). Hydrochemical study of Shatt Al-Arab water in Basra City. *Nature Environment and Pollution Technology, 10*(1), 17–23. https://doi.org/10.5958/2394-448X.2021.00012.2
[2] A l-Hashmi, X., Al-Janabi, H., Abbas, S., & Kareem, R. (2023). Integrating WQI and GIS to assess water quality in Shatt Al-Hillah River, Iraq using physicochemical and heavy metal elements. Applied Water Science, 13, 147
[3] Al-Aboodi, A. H.; Abbas, S. A. and Ibrahim, H. T. (2018). Effect of Hartha and Najibia power plants on water quality indices of Shatt Al-Arab River, south of Iraq. Applied Water Science, 8, (64):
[4] Al-Asadi, S.A.R.; Al-Qurnawi, W.S.; Al Hawash, A.B.; Ghalib, H.B. and Alkhlifa, H.A
[5] . (2020). Water quality and impacting factors on heavy metals levels in Shatt Al-Arab River, Basra, Iraq. Appl WaterSci.10(5):1–15.
[6] Al-Silawy, Z. H., Al-Abbawy, D. A., & Al-Mahmood, H. K. H. (2025). *Assessment of*
[7] *seasonal and spatia variation of heavy metals concentrations in Shatt Al-Arab River, Basrah, Iraq. EnvironmentAsia, 18(2), 131–143l*
[8] APHA. (2017). standard method for the examination of water and waste water: (American public Health Association) 23rd edition Washington, DC
[9] Hamzah, Z. A. H. (2025). Water quality of the Shatt Al-Arab River evaluation using the Nemerow pollution index method. Advances in Science and Technology Research Journal, 19(5), 14–20.
[10] Jaber, H.S. (2012). A Geographic Information System application for water resources of Iraq. Journal of Engineering and Development, 16(1): 23-31.
[11] Jassim, I.N. and Al-Amiri, N.J. (2023). Indicate the pollution extent at Shatt Al-Arab waters by water quality index (Canadian model). Journal of Survey in Fisheries Sciences 10(3S): 2737-2754J. https://doi.org/10.24996/ijs.2023.64.9.12
[12] Kumar, R., Singh, R.D. and Sharma, D. (2005) .Water recourses of India. *Current Science,* 89 (5): 794-811.
[13] Mehasin Gh. Hashim , Amjed K. Resen , Mujtaba A.T. Ankush, (2025). Evaluation of Water Quality in the Northern Region of the Shatt al-Arab River, Southern Iraq , Egyptian Journal of Aquatic Biology & Fisheries Zoology Department, Faculty of Science, Ain Shams University, Cairo, Egyp Vol. 29(1): 187 – 202
[14] Mohamed, A.R.M.; Sadek A.; Hussein,S.A. ; Laith F. and Lazem,L.F. (2016) .Appraisal of Some Water Quality Criteria of the Shatt Al-Arab River by Applying Geographical Information System (GIS). Global Journal of Biology, Agriculture and Health Sciences, 5(3):43-53.
[15] Mohammed, A. A. and Al Chalabi, A. S. (2022). Environmental Impact Assessment Study for Shatt Al-Arab River Receiving Industrial Wastewater. Basrah Journal for Engineering Sciences, 22 (1): 93- 98.
[16] Moyel, M.S. (2014). Assessment of water quality of the Shatt al-Arab river, using multivariate statistical technique. Mesopotamia Environment Journal, 1(1), 39-46.
[17] Qzar, I.A.; Al-Hejuje, M.M.; Talib, A. & Rajab, A.M. (2021). The effect of regulations and Standards for drinking-water quality river water quality for agricultural irrigation: resources of Iraq. Journal of Engineering and International Journal of Development, 16(1): 23-31. 104 pp
[18] WHO(world Health Organization).(2018).Aglobal overview of national regulations and Standards for drinking-water quality:104 pp.
[19] Yasmin, R., Islam, M. & Alam, M. J.(2012).A Study on Potential Application of Geographic Information Systems (GIS) in Fisheries and Aquaculture of Bangladesh. *World J. Fish and Marine Sci.*, 4 (6): 609-619.
[20] Al-Nour, A. J. M. (2021). Determination of the most influential water quality parameters and evaluation of irrigation suitability for wheat (Triticum aestivum L.). MSc Thesis, College of Agriculture, University of Basrah, Iraq.

[21] Al-Ghalibi, M. Q. N., & Al-Saadi, S. A. A. R. (2019). Distribution of salts in the waters of the Shatt Al-Arab River. *Arabian Gulf Journal*, 47(3–4), 234–257.

[22] Al-Issa, S. A. A. (2004). Ecological study of aquatic plants and their attached algae in the Shatt Al-Arab River. PhD Dissertation, College of Agriculture, University of Basrah, Iraq.

[23] Adlan, N. H. (2022). Ecological study of aquatic plants and water quality in the Shatt Al-Arab River using Geographic Information Systems (GIS). PhD Dissertation, College of Science, University of Basrah, Iraq.

[24] Al-Bazouni, A. J. A. (2023). Mathematical modeling and field measurements of discharge effects on chemical properties and saltwater intrusion in the Shatt Al-Arab River. PhD Dissertation, College of Agriculture, University of Basrah, Iraq.

[25] Al-Asadi, S. A. A., & Al-Lami, I. K. (2014). Some environmental impacts of tidal phenomena in the Shatt Al-Arab, southern Iraq. *Proceedings of the Seventh Scientific Conference, University of Wasit*, Iraq.

[26] Al-Zubaidi, I. N. J. (2023). Water quality assessment and pollution status of the Shatt Al-Arab River and its suitability for irrigation using the Canadian Water Quality Index. PhD Dissertation, College of Agriculture, University of Basrah, Iraq.

[27] Al-Taher, S. M. A. R. (2019). Water quality assessment and application of trophic status and river pollution indices in the northern part of the Shatt Al-Arab River. MSc Thesis, College of Science, University of Basrah, Iraq.

[28] Al-Eidawi, H. T. A. (2021). Spatial variation of the Shatt Al-Arab River estuarine zone, southern Iraq. MSc Thesis, College of Education for Human Sciences, University of Basrah, Iraq.

[29] Zhao, Y., Liu, J., Chen, X., Wang, H., Li, Z., & Zhang, Q. (2024). Groundwater sulfate in the Pearl River Delta driven by urbanization: Spatial distribution, sources and factors. *Applied Geochemistry, 156*, 105766. https://doi.org/10.1016/j.apgeochem.2023.105766